

Supporting information

**Low-frequency multiplex CARS microscopy with a high-repetition near-infrared supercontinuum laser**

Yusuke Arashida<sup>1</sup>, Atsushi Taninaka<sup>1,2</sup>, Takahiro Ochiai<sup>1,2</sup>, Hiroyuki Mogi<sup>1</sup>, Shoji Yoshida<sup>1</sup>, Masamichi Yoshimura<sup>3</sup>, Osamu Takeuchi<sup>1</sup>, and Hidemi Shigekawa<sup>1</sup>

<sup>1</sup>Faculty of Pure and Applied Sciences, University of Tsukuba, Tsukuba 305-8573, Japan

<sup>2</sup>TAKANO Co., LTD., Miyada-mura, Kamiina-gun, Nagano, 399-4301 Japan

<sup>3</sup>Graduate School of Engineering, Toyota Technological Institute, Hisakata, Tempaku, Nagoya 468-8511, Japan

## 1. Spectral shape caused by the interference between CARS and NRB

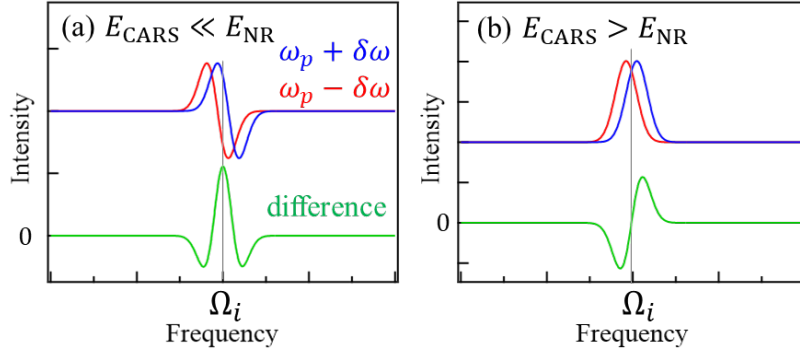


Fig. S1 Schematics of typical interference spectra with CARS and NRB. Red and blue curves represent spectra for slightly different  $\omega_p$  ( $\pm \delta\omega$ ) values assuming (a)  $E_{\text{CARS}} \ll E_{\text{NR}}$  and (b)  $E_{\text{CARS}} > E_{\text{NR}}$ . The blue and red lines are spectra for slightly different  $\omega_p$ , and when the difference between the spectra is considered, a peak appears at the vibration frequency  $\Omega_i$  as shown by the green line. The green curves show the difference between red and blue curves. When  $E_{\text{CARS}}$  has a resonance peak shape and  $E_{\text{NR}}$  is a non-phase-sensitive background, the spectrum with the Fano shape appears when the NRB amplitude is sufficiently larger than the CARS signal as shown in (a). On the other hand, when the effect of interference by NRB is small, a spectrum with a peak appears as shown in (b). Then, when the difference between the two spectra obtained by changing  $\omega_p$  is considered, the spectrum has a structure with the largest slope at the frequency  $\Omega_i$ . To obtain an accurate Raman shift, it is necessary to consider fitting with the degree of interference. Even if the effect of interference NRB is small, the background can be set to 0 by considering the difference, which is useful for extracting CARS signals. However, depending on the degree of interference, a spectral shape between those in (a) and (b) may appear for the data.

## 2. Confirmation of wide bandwidth

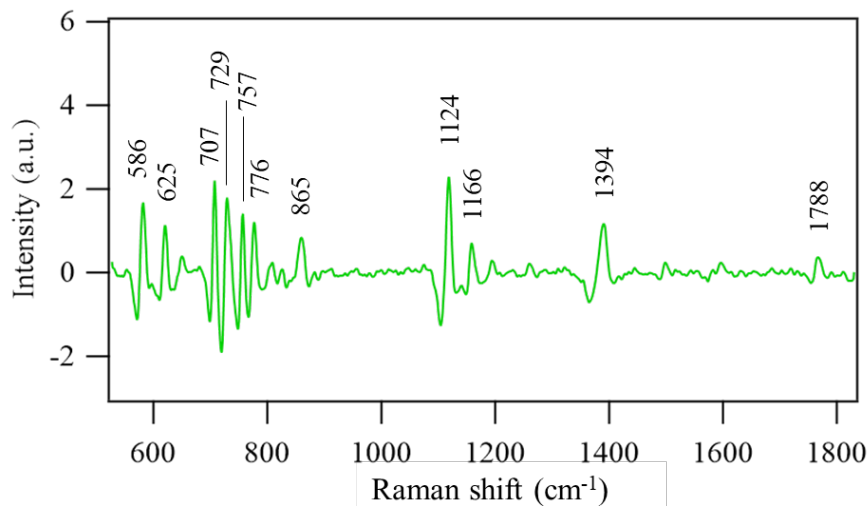


Fig. S2 **Broadband CARS spectrum of a polyimide film.** The spectrum was obtained as the difference between the two spectra measured for  $\lambda_p \pm 0.2$  nm ( $\delta\lambda = 0.4$  nm), as shown in Figs. 1 (d) and 1 (e). According to previous studies<sup>23-25</sup>, the peak at 1788 cm<sup>-1</sup> is originated from the stretching vibration of the C-CO-C structure. The peak at 1394 cm<sup>-1</sup> and 1124 cm<sup>-1</sup> are from the stretching and the bending vibration of the C-N-C structure, respectively. The multiple peaks observed in the region from 707 cm<sup>-1</sup> to 776 cm<sup>-1</sup> are considered to be oscillations due to the dianhydride structure. The peaks found at 865 cm<sup>-1</sup>, 625 cm<sup>-1</sup>, and 586 cm<sup>-1</sup> are vibrations of diamine ring breathing, C-O-C bonding, and monosubstituted benzene deformation, respectively.

### 3. Chirp of the supercontinuum laser

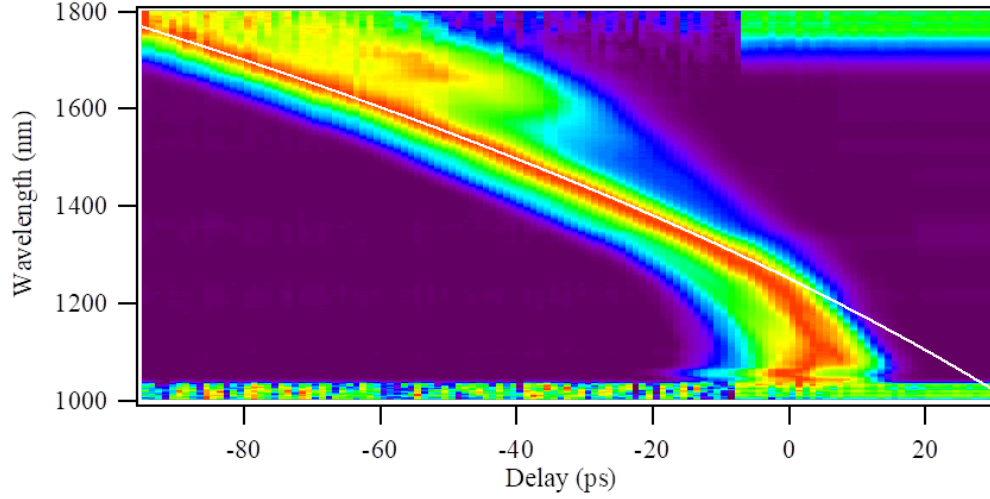


Fig. S3 Wavelength dependence of group delay of  $\omega_s$  measured by frequency-resolved optical gating (FROG). Spectra of the sum-frequency generation (SFG) between the  $\omega_p$  and  $\omega_s$ , which is generated by using a BBO crystal, were measured by changing the optical delay between the two beams of  $\omega_p$  and  $\omega_s$ . The wavelength  $\lambda_s$  of the vertical axis was calculated by  $1/\lambda_s = 1/\lambda_{\text{SFG}} - 1/\lambda_p$  considering the wavelength of  $\omega_p$  for the wavelength of sum-frequency light in the visible light region.

#### 4. Spot size of the beams on the sample

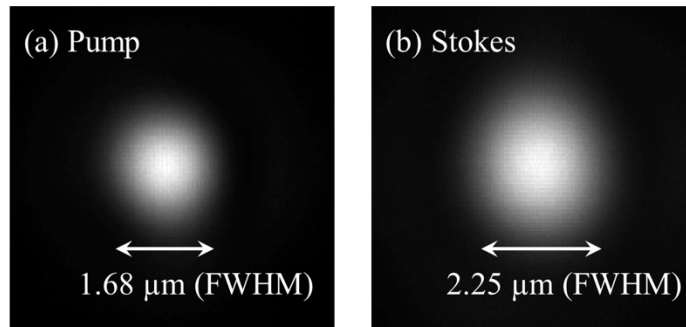


Fig. S4, the spot size of the pump and the Stokes beams on the focal plane measured with optical microscope with the magnitude of  $\times 100$  and using Si-based image sensor (ASI 294MC, ZWO).

## 5. Spatial resolution of CARS imaging

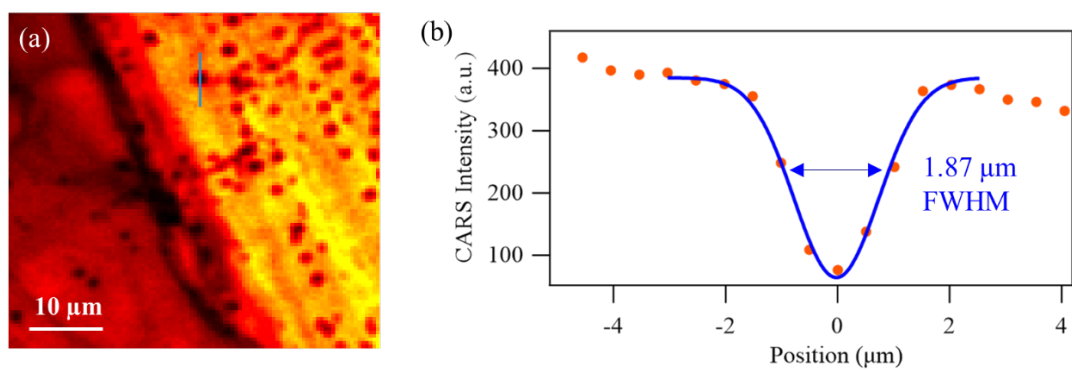
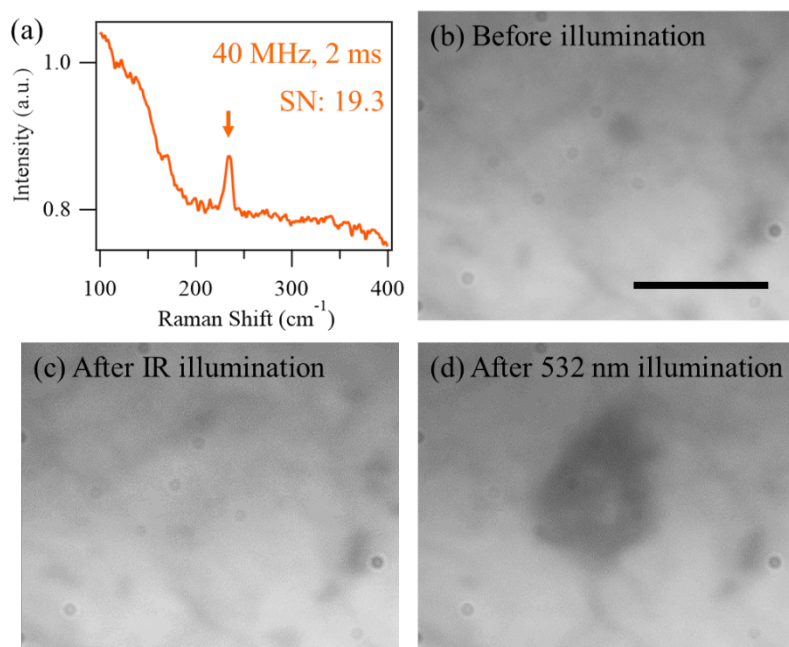


Fig. S5 As an estimate of spatial resolution, the smallest spatial shape change of CARS signal imaging in Fig. 4 was used for evaluation. (a) CARS image depicted from Fig. 4 in the text. (b) The red dots show the cross section along the blue line in (a). The blue curve shows the result of Gaussian fitting of the cross section. The spatial resolution of our CARS is evaluated to  $1. \mu\text{m}$  by using the upper limit of the fitting result of  $\text{FWHM} = 1.78 \pm 0.09 \mu\text{m}$ .

## 6. Other advantages of the developed system



**Fig. S6 High efficiency of the developed system and a damage induced by laser illumination.** (a) Raw spectrum of the sulfur crystal sample with an exposure time of 2 ms, a repetition frequency of 40 MHz, and the power of 60 mW. Optical microscopy images of sample obtained (b) before and (c) after the illumination with the IR laser. (d) Optical microscope image after illumination with a visible laser with a wavelength of 532 nm with the power of 60 mW. The black bar denotes 5  $\mu\text{m}$ .

The sulfur crystal was used as the sample, and the laser repetition frequency was set to 40 MHz. Figure 4S shows the results obtained with an exposure time of 2 ms. A Raman signal with a 220 cm<sup>-1</sup> peak clearly observed with an SN ratio of about 19. By IR excitation multiplex CARS, we achieved the same high measurement efficiency as that in previous research using visible light excitation, even on the low-wavenumber side of

the fingerprint region<sup>14</sup>. This microscopy is expected to enable the effective tracking of molecules containing heavy atoms and polymers.

Optical microscopy images of the sample obtained before and after the measurement of the data shown in Fig. S5a are shown in Figs. S5b and S5c, respectively. There are no major differences between the two images. Next, in the optical system shown in Fig. 1, the LPF was replaced with a BPF of  $532 \pm 10$  nm. Then, the obtained visible light was set to the same power as the IR (60 mW) and irradiated to the same part of the sample. As shown in Fig. S6d, the optical contrast changed. Since visible light has a higher absorption rate than IR, the sample is considered to have been damaged. Namely, IR excitation could induce CARS while suppressing the sample damages caused by light irradiation, as expected.

## 7. Optical microscopy images of the phase transition of S crystal.

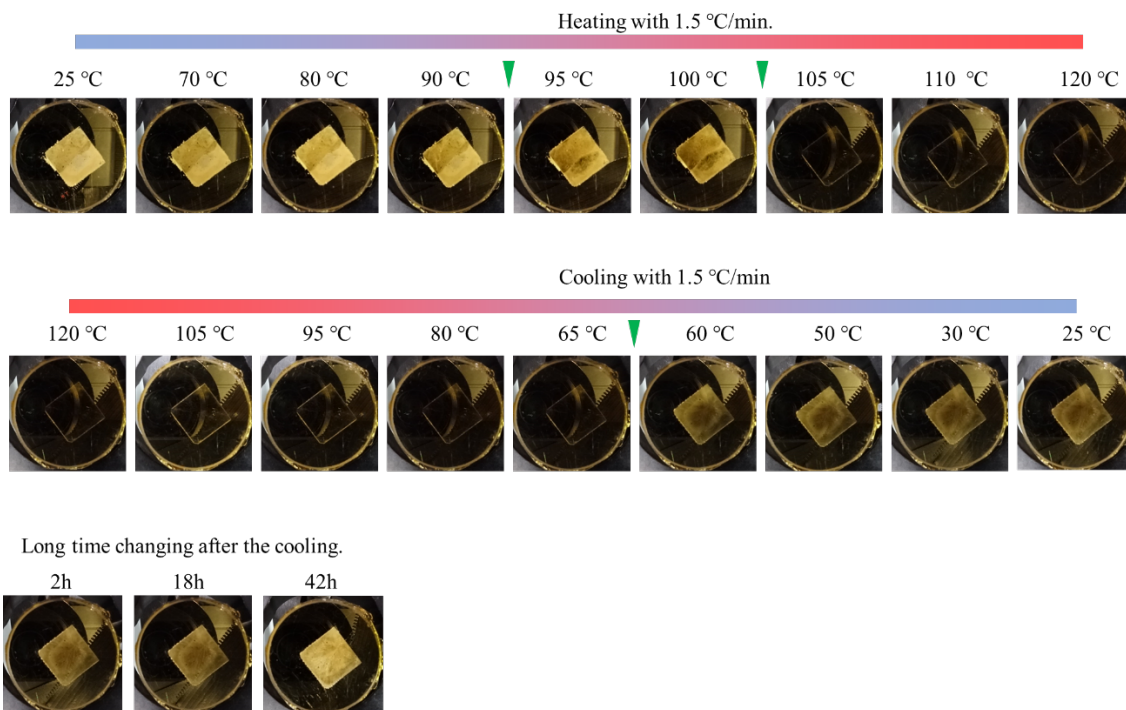


Fig. S7 Pictures of the sulfur crystal sample sandwiched between a sapphire plate and a gold mirror. Temperature dependence of the phase transition during heating and cooling are shown. The green arrows denote the points where phase transitions appeared.